

Electronic supplementary information

Bi-functional sterically hindered phenol lipid-based delivery systems as potential multi-target agents against Alzheimer's disease via intranasal route

Evgenia A. Buriilova,^a Tatiana N. Pashirova,^{*a} Irina V. Zueva,^a Elmira M. Gibadullina,^a Sofya V. Lushchekina,^b Anastasia S. Sapunova,^a Ramilya M. Kayumova,^c Alexey M. Rogov,^c Vladimir G. Evtjugin,^c Igor A. Sudakov,^a Alexandra B. Vyshtakalyuk,^a Alexandra D. Voloshina,^a Sergey.V. Bukharov,^d Alexander R. Buriilov,^a Konstantin A. Petrov,^a Lucia Ya. Zakharova,^a Oleg G. Sinyashin^a

^a*Arbuzov Institute of Organic and Physical Chemistry, FRC Kazan Scientific Center of RAS, Arbuzov St., 8, Kazan, 420088, Russian Federation*

^b*N.M. Emanuel Institute of Biochemical Physics of Russian Academy of Sciences, Kosygina str. 4, Moscow 119334, Russian Federation*

^c*Kazan Federal University, Kremlyovskaya St., 18, Kazan, 420008, Russia*

^d*Kazan National Research Technological University, Karl Marx str., 68, 420015 Kazan, Russian Federation*

***Corresponding authors:**

Tatiana N. Pashirova, Arbuzov Institute of Organic and Physical Chemistry, FRC Kazan Scientific Center of RAS, Arbuzov str. 8, Kazan, 420088, Russian Federation, tel: (007) 843 273 22 93, fax: (007) 843 273 22 53,
E-mail: tatyana_pashirova@mail.ru

Contents

Fig. S 1. Spectra and calibration curve of SHP-2-R in Saline	S3
Table S1. hAChE and hBChE inhibitory activity of SHP-n-R	S4
Fig. S2. Interactions of the compound SHP-2-C16 (carbon atoms are shown cyan) with hAChE. (C, D) Example of position of the ligand SHP-2-C16 in the PAS.	S5
Fig. S3. Surface tension isotherms of SHP-s-R	S6
Fig. S4. The dependences of the specific conductivity of SHP-s-R on their concentration	S7
Fig. S5. Absorption profile of Orange OT in the presence of increasing SHP-s-R concentration	S8
Fig. S6. Absorbance Orange OT on SHP-s-R concentrations	S9
Fig. S7. Fluorescence spectra of pyrene in SHP-s-R solutions	S10
Fig. S8. Dependence of the intensity ratio (I_1/I_3) of the first and third peaks of pyrene on SHP-s-R concentrations	S11
Fig. S9. Fluorescence of pyrene in SHP-2-R solutions in the absence and in the presence of CPB; dependence of $\ln(I_0/I)$ in SHP-2-R solutions on CPB concentrations	S12
Table S2. Hemolytic action against human red blood cells of SHP-s-R	S13
Table S3 Size, using number, intensity and volume distribution in analysis, Z–Average, polydispersity index and Zeta potential of lipid formulations.	S14
Fig. S10. Spectra of SHP-2-10 and SHP-2-16 in Saline (NaCl, 0.15 M) recorded during release time	S15
Table S4. Hemolytic action against human red blood cells of SHP-s-R-loaded lipid formulations	S16
Fig. S11. Chemiluminescence intensity for ABAP and LM in a buffer solution with the addition of test compounds	S17
Fig. S12. Chemiluminescence intensity for ABAP and LM in a buffer solution with the addition of SHP-2-R-loaded lipid formulations	S18

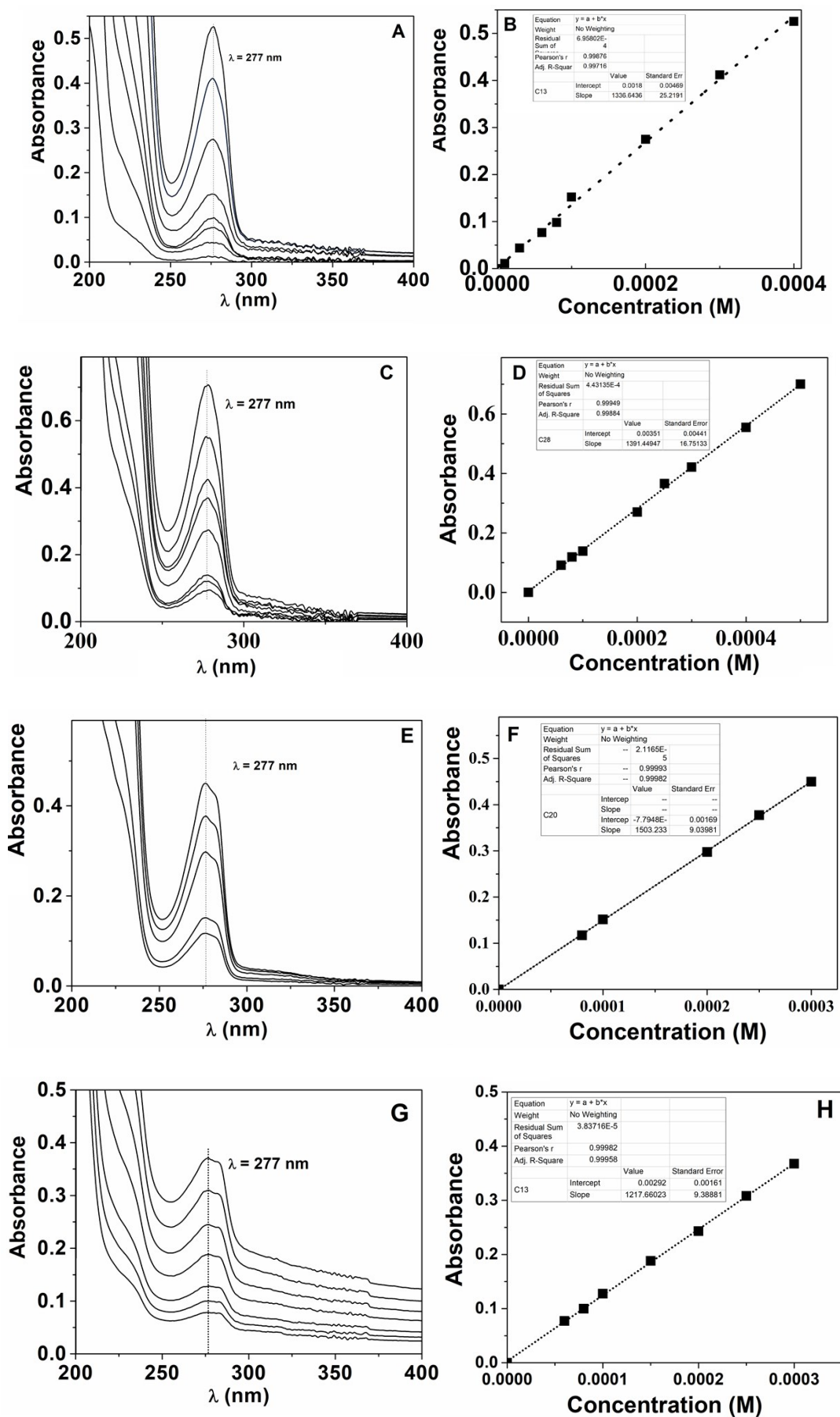


Fig. S1. Spectra (A, C, E, G) and calibration curve (B, D, F, G) of SHP-2-8 (A, B), SHP-2-10 (C, D), SHP-2-12 (E, F), SHP-2-16 (G, H) in Saline (NaCl, 0.15 M), pH=7.4, L=1 cm, 25°C.

Table S1. hAChE and hBChE inhibitory activity of SHP-n-R

Compounds	IC ₅₀ (μM)		S ratio hAChE/hBChE
	hAChE	hBChE	
SHP-2-Bn ^a	200.0 ± 50	20.0 ± 0.1	10
SHP-2-8	30±0.0	6.5±0.5	4.6
SHP-2-10	3.12±0.42	3.16±0.09	1
SHP-2-12	1.2±0.07	16.7±0.33	0.07
SHP-2-16	0.33±0.2	10±0.0	0.03
SHP-3-Bn ^a	75 ± 5	40 ± 0.1	1.9
SHP-3-8	3.04±0.15	2.76±0.39	1
SHP-3-10	3.32±0.16	3.4±0.26	1
SHP-3-12	9.23±0.46	147±0.41	0.06
SHP-3-16	> 200	> 200	1

^adata from ⁴⁰

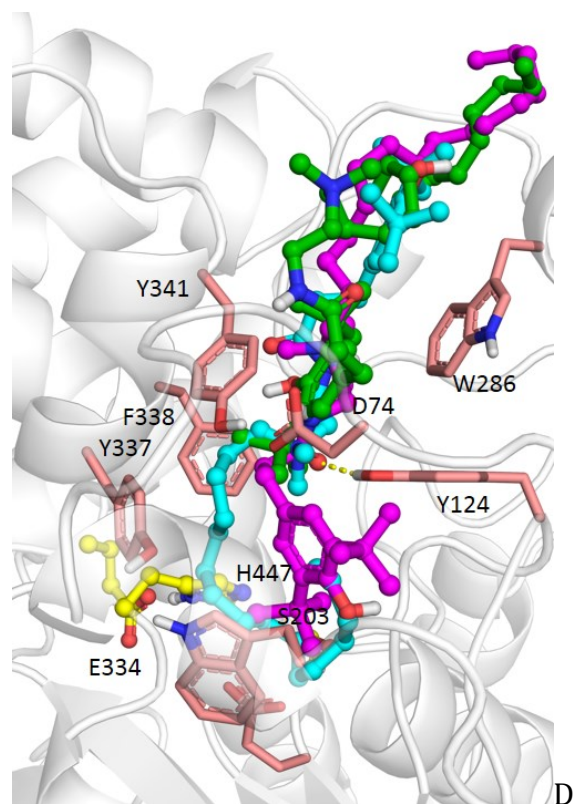
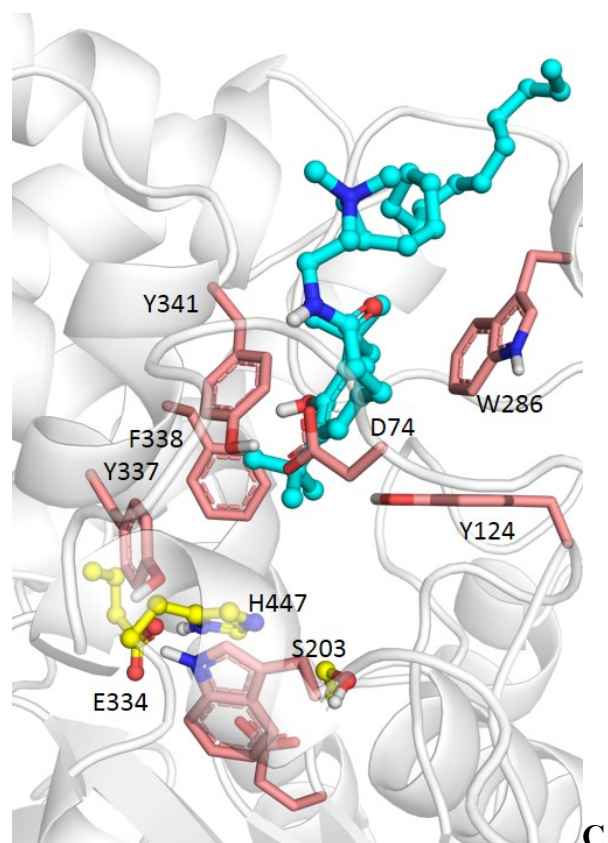


Fig. S2. Interactions of the compound SHP-2-C16 (carbon atoms are shown cyan) with hAChE. (C, D) Example of position of the ligand SHP-2-C16 in the PAS.

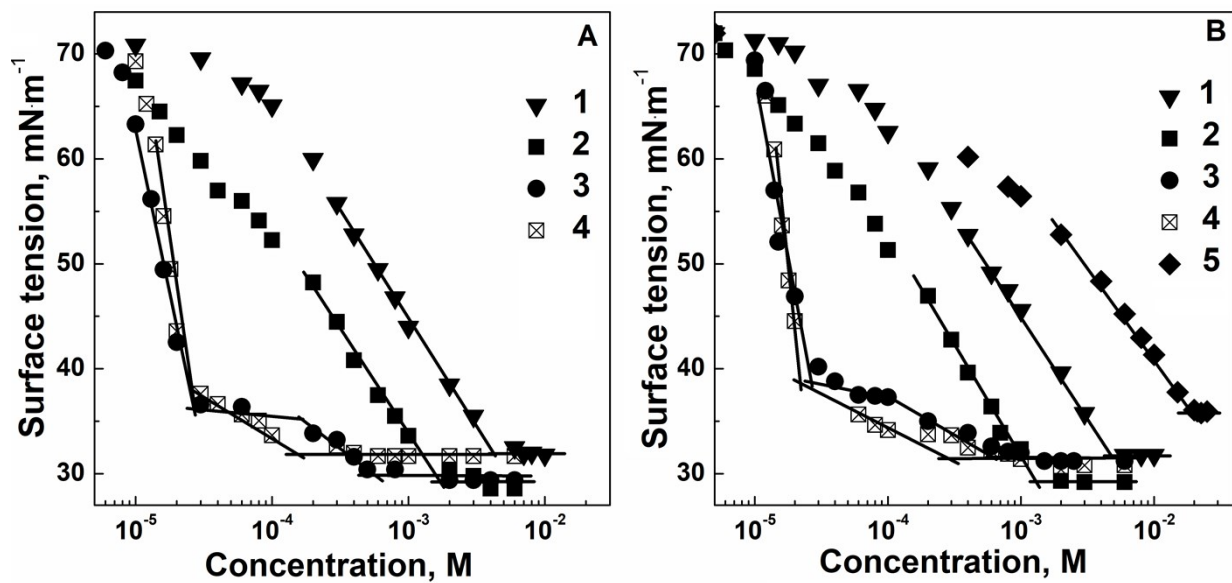


Fig. S3. Surface tension isotherms of SHP-2-R (A), SHP-3-R (B) solutions at 25 °C, where SHP-s-8 (1), SHP-s-10 (2), SHP-s-12 (3), SHP-s-16 (4), SHP-3-Bn (5), 25 °C.

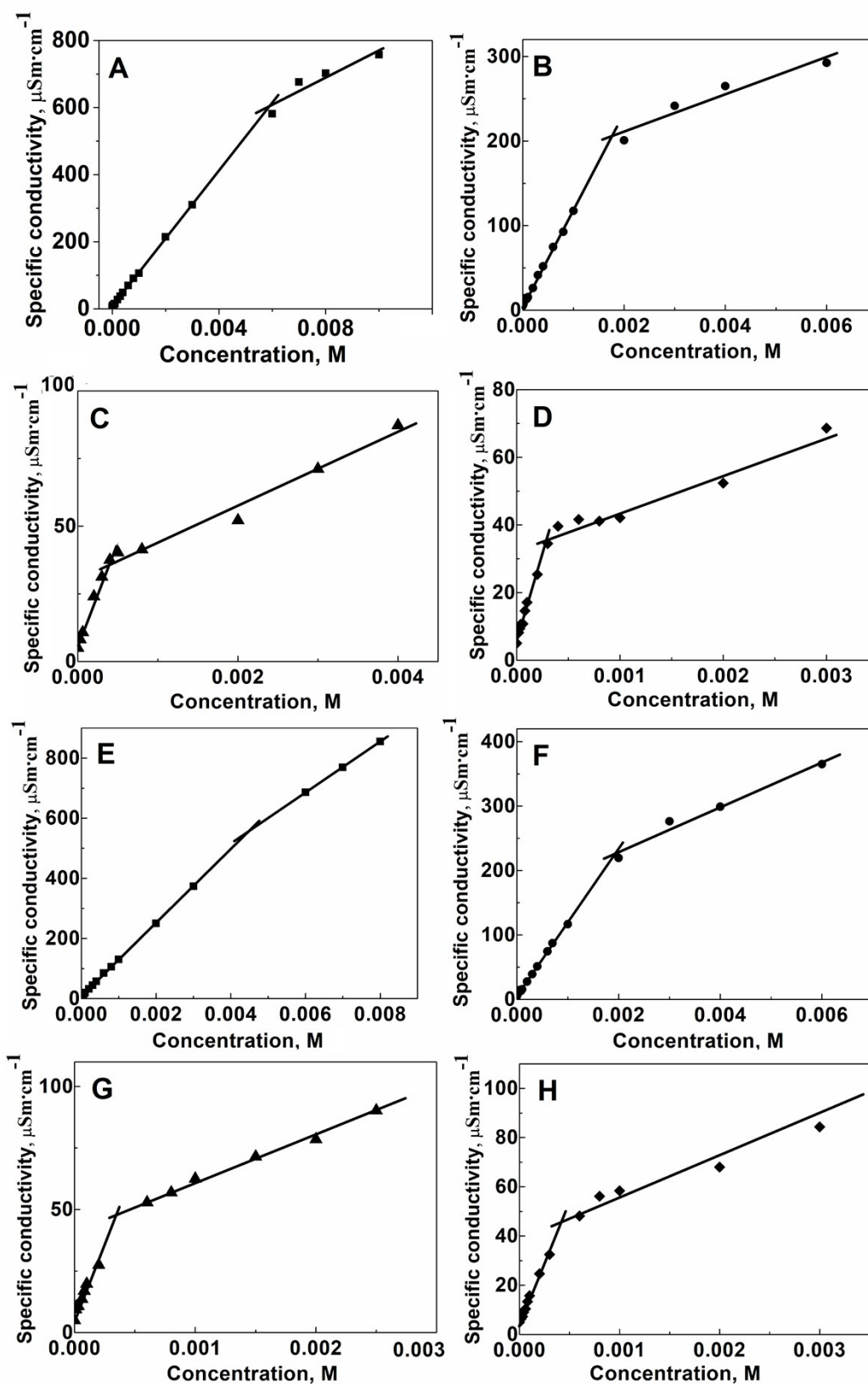


Fig. S4. The dependences of the specific conductivity of SHP-s-R on their concentration, where SHP-2-8 (A), SHP-2-10 (B), SHP-2-12 (C), SHP-2-16 (D), SHP-3-8 (E), SHP-3-10 (F), SHP-3-12 (G), SHP-3-16 (H) at 25 °C.

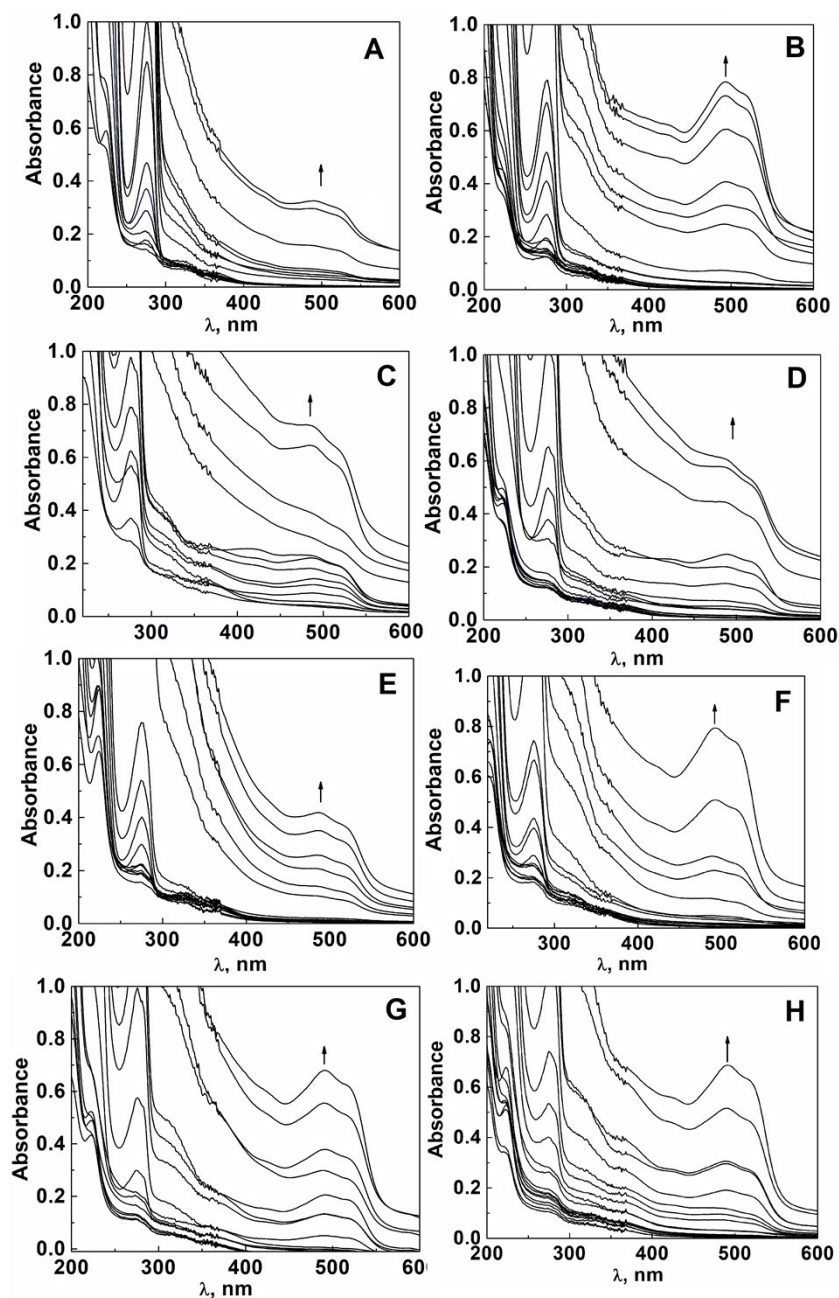


Fig. S5. Absorption profile of Orange OT in the presence of increasing SHP-s-R concentration, where SHP-2-8 (A), SHP-2-10 (B), SHP-2-12 (C), SHP-2-16 (D), SHP-3-8 (E), SHP-3-10 (F), SHP-3-12 (G), SHP-3-16 (H), $L = 1\text{ cm}$, $\lambda = 490\text{ nm}$, 25°C , $C_{\text{SHP-2-8}}$ (mM): 0.01, 0.03, 0.06, 0.08, 0.1, 0.2, 0.3, 0.4, 0.8, 1, 2, 3, 4, 5, 6, 7, 7.5; $C_{\text{SHP-2-10}}$ (mM): 0.01, 0.015, 0.02, 0.03, 0.04, 0.06, 0.08, 0.1, 0.2, 0.3, 0.4, 0.6, 0.8, 1, 2, 2.5, 3, 3.5, 4, 5; $C_{\text{SHP-2-12}}$ (mM): 0.06, 0.2, 0.3, 0.4, 0.5, 0.6, 0.8, 1, 1.5, 2, 2.5, 3, 4, 6; $C_{\text{SHP-2-16}}$ (mM): 0.01, 0.012, 0.014, 0.016, 0.018, 0.02, 0.03, 0.04, 0.06, 0.1, 0.2, 0.3, 0.4, 0.6, 0.8, 1, 2, 2.5, 3; $C_{\text{SHP-3-8}}$ (mM): 0.01, 0.015, 0.03, 0.04, 0.06, 0.08, 0.1, 0.2, 0.3, 0.4, 0.6, 3, 4, 5, 5.5, 6, 6.5; $C_{\text{SHP-3-10}}$ (mM): 0.006, 0.01, 0.02, 0.03, 0.04, 0.08, 0.1, 0.2, 0.3, 0.4, 0.6, 0.7, 1.5, 2, 2.5, 3, 3.5, 4.5; $C_{\text{SHP-3-12}}$ (mM): 0.01, 0.02, 0.03, 0.04, 0.05, 0.08, 0.1, 0.2, 0.4, 0.6, 0.8, 1, 1.5, 2, 2.5, 3; $C_{\text{SHP-3-16}}$ (mM): .01, 0.012, 0.014, 0.016, 0.018, 0.02, 0.03, 0.04, 0.06, 0.08, 0.1, 0.2, 0.3, 0.4, 0.6, 0.8, 1, 1.5, 2.

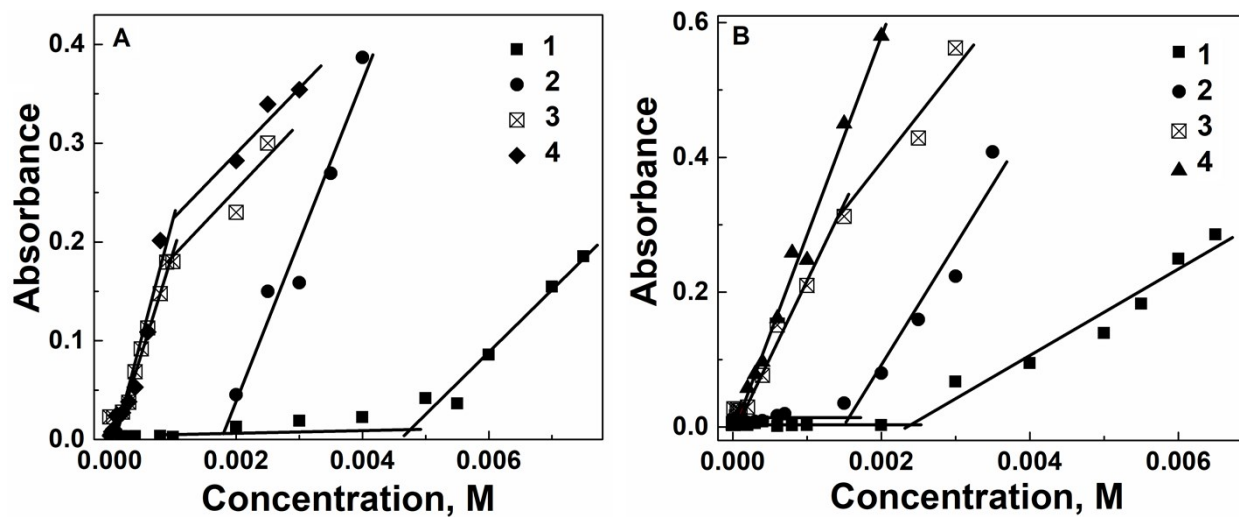


Fig. S6. Absorbance Orange OT on SHP-2-R (A) and SHP-3-R (B) concentrations, where SHP-s-8 (1), SHP-s-10 (2), SHP-s-12 (3), SHP-s-16 (4), at $\lambda=490$ nm, $L=1$ cm, 25 °C.

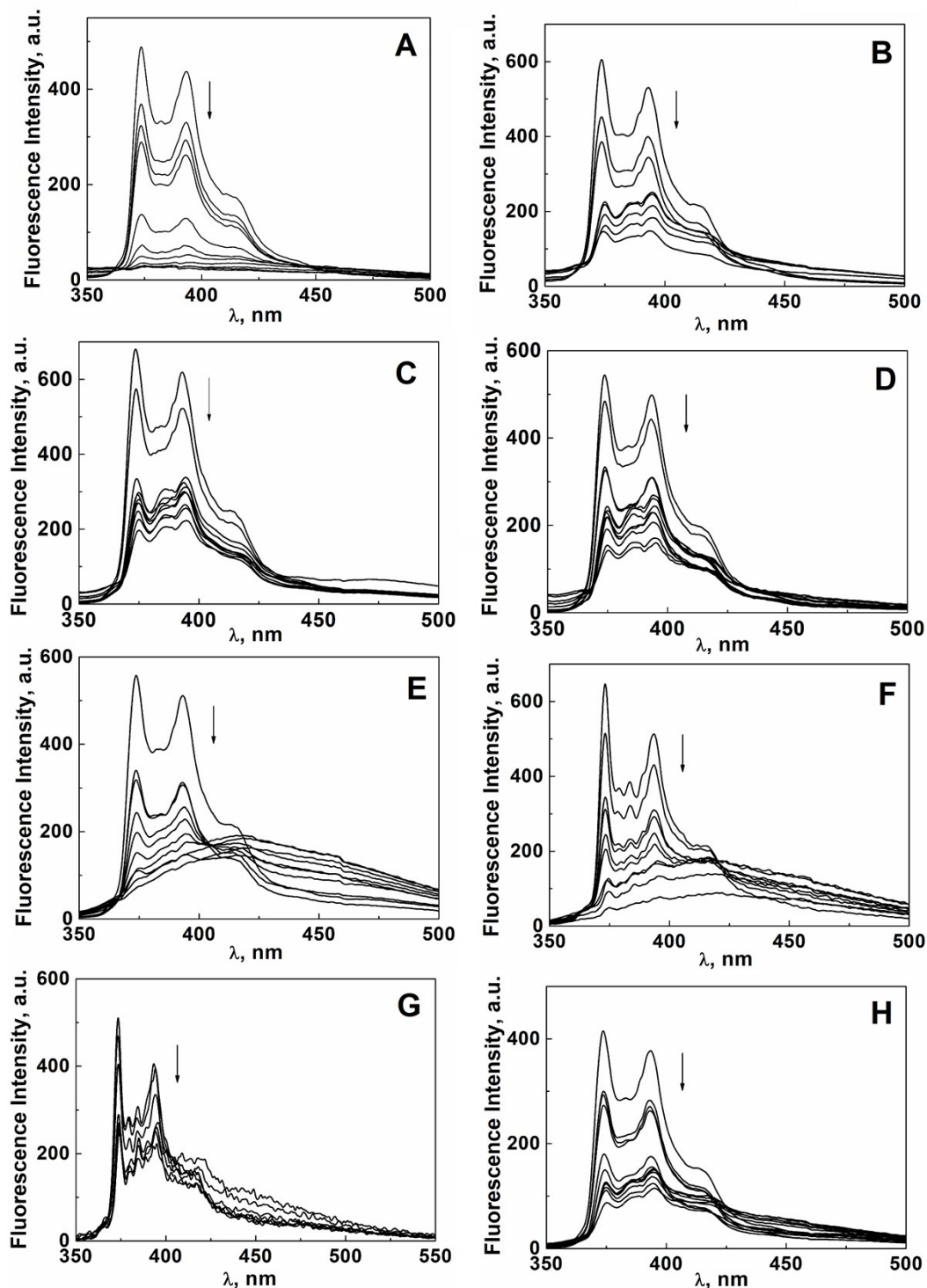


Fig. S7. Fluorescence spectra of pyrene in SHP-s-R solutions, where SHP-2-8 (A), SHP-2-10 (B), SHP-2-12 (C), SHP-2-16 (D), SHP-3-8 (E), SHP-3-10 (F), SHP-3-12 (G), SHP-3-16 (H), 25 °C, $C_{\text{SHP-2-8}}$ (mM): 0.4, 0.6, 1, 2, 3, 4, 5, 6, 7, 8; $C_{\text{SHP-2-10}}$ (mM): 0.4, 0.6, 0.8, 2, 3, 4, 5, 6; $C_{\text{SHP-2-12}}$ (mM): 0.03, 0.05, 0.2, 0.3, 0.4, 0.5, 0.8, 1, 2, 2.5; $C_{\text{SHP-2-16}}$ (mM): 0.04, 0.06, 0.08, 0.1, 0.2, 0.3, 0.4, 0.6, 0.8, 1, 1.5, 2; $C_{\text{SHP-3-8}}$ (mM): 0.08, 0.1, 0.2, 0.4, 0.6, 0.8, 2, 3, 4, 5; $C_{\text{SHP-3-10}}$ (mM): 0.2, 0.4, 0.6, 0.7, 0.9, 1, 2, 3, 4, 6; $C_{\text{SHP-3-12}}$ (mM): 0.1, 0.14, 0.2, 0.24, 0.34, 0.4, 0.6, 0.8; $C_{\text{SHP-3-16}}$ (mM): 0.02, 0.04, 0.06, 0.08, 0.1, 0.2, 0.4, 0.6, 0.7, 0.8, 1, 2.

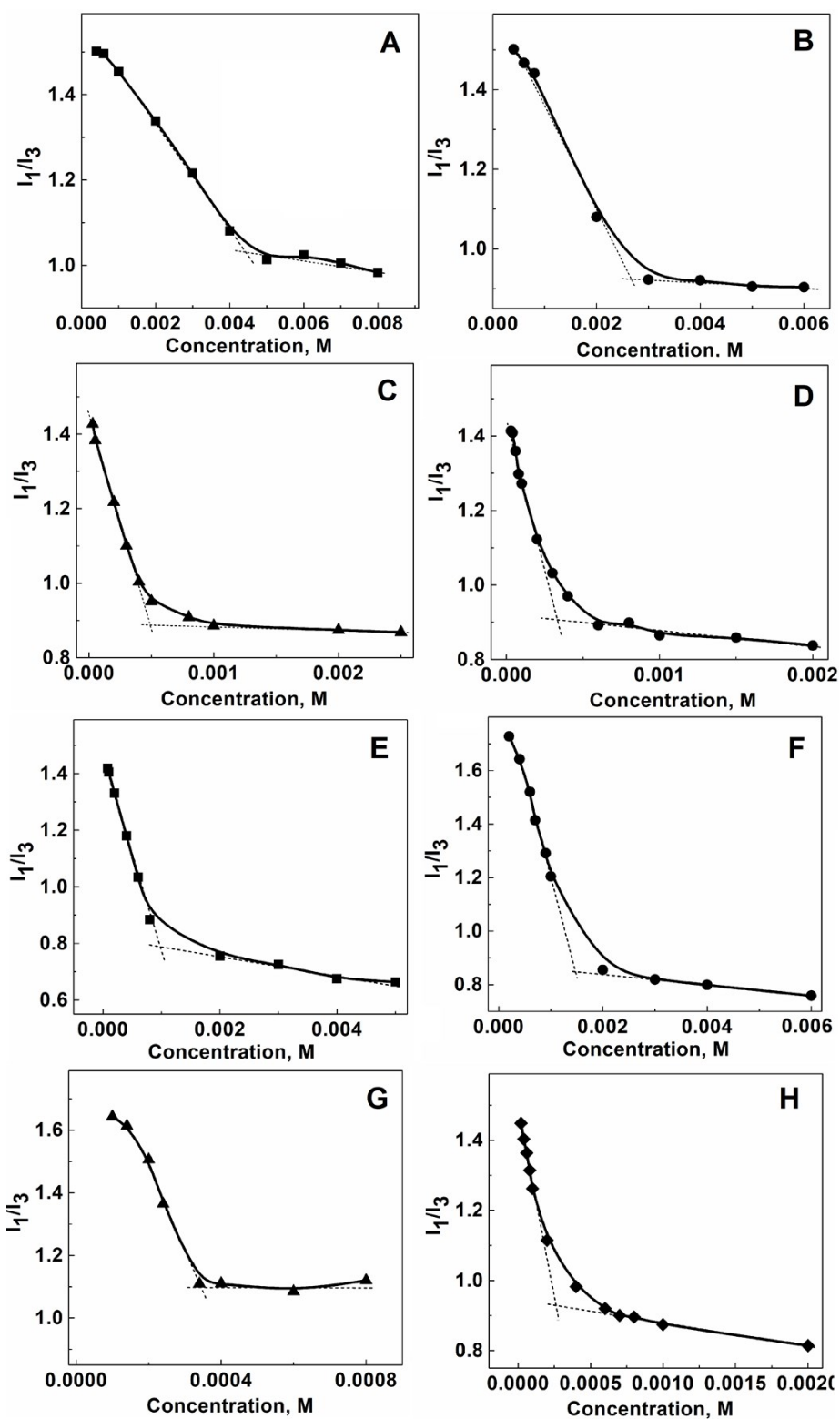


Fig. S8. Dependence of the intensity ratio (I_1/I_3) of the first and third peaks of pyrene on SHP-s-R concentrations where SHP-2-8 (A), SHP-2-10 (B), SHP-2-12 (C), SHP-2-16 (D), SHP-3-8 (E), SHP-3-10 (F), SHP-3-12 (G), SHP-3-16 (H), 25 °C.

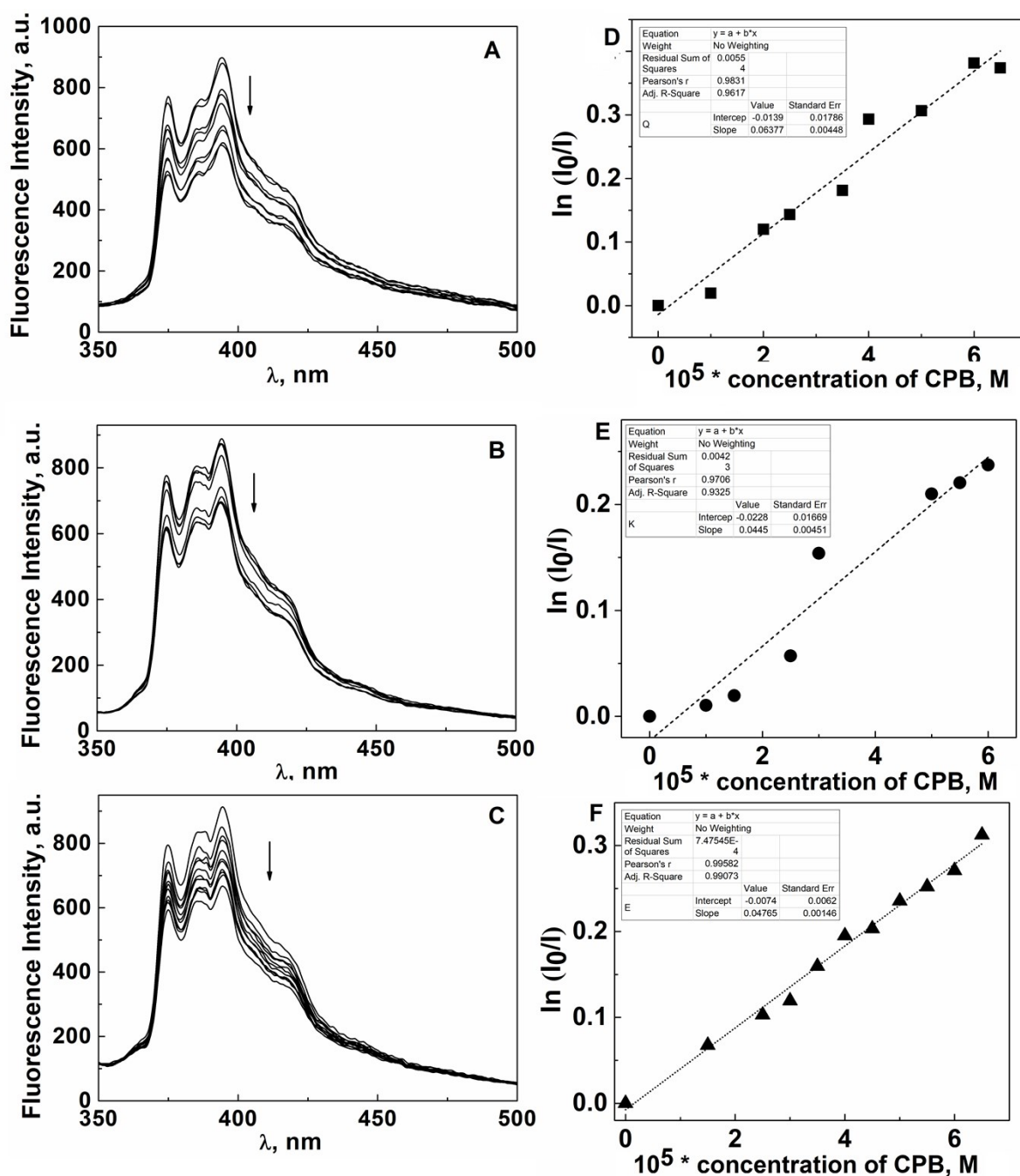


Fig. S9. Fluorescence of pyrene in SHP-2-10 (A), SHP-2-12 (B), SHP-2-16 (C) solutions in the absence and in the presence of CPB; dependence of $\ln(I_0/I)$ in SHP-2-10 (D), SHP-2-12 (E), SHP-2-16 (F) solutions on CPB concentrations, $\lambda=394$ nm. A, D: $C_{\text{SHP-2-10}} = 3\text{mM}$, $C_{\text{CPB}} (\text{M}) = 1 \times 10^{-5}, 2 \times 10^{-5}, 2.5 \times 10^{-5}, 3.5 \times 10^{-5}, 4 \times 10^{-5}, 5 \times 10^{-5}, 6 \times 10^{-5}, 6.5 \times 10^{-5}$; B, E: $C_{\text{SHP-2-12}} = 1\text{mM}$, $C_{\text{CPB}} (\text{M}) = 1 \times 10^{-5}, 1.5 \times 10^{-5}, 2.5 \times 10^{-5}, 3 \times 10^{-5}, 5 \times 10^{-5}, 5.5 \times 10^{-5}, 6 \times 10^{-5}$; C, F: $C_{\text{SHP-2-16}} = 2\text{mM}$, $C_{\text{CPB}} (\text{M}) = 1.5 \times 10^{-5}, 2.5 \times 10^{-5}, 3 \times 10^{-5}, 3.5 \times 10^{-5}, 4 \times 10^{-5}, 4.5 \times 10^{-5}, 5 \times 10^{-5}, 5.5 \times 10^{-5}, 6 \times 10^{-5}, 6.5 \times 10^{-5}$;

Table S2

Hemolytic action against human red blood cells of SHP-s-R

Compounds	Hemolysis, %							HC ₅₀ , μM
	Concentration, μM							
	2	7	10	50	200	600	1000	
SHP-2-8	0.1±0.01	0.4±0.03	0.9±0.08	3.4±0.3	37.4±3.2	84.7±8.1	98.3±8.2	267.4±21.1
SHP-2-10	0.4±0.03	0.9±0.08	2.2±0.2	52.0±5.0	59.3±5.4	66.2±5.9	79.9±7.1	48.1±3.8
SHP-2-12	0.2±0.02	1.7±0.1	3.4±0.3	38.6±3.3	77.5±6.9	71.7±6.5	75.5±6.4	64.8±5.6
SHP-2-16	0.2±0.02	0.8±0.07	2.10±0.17	45.7±3.5	61.5±5.1	73.6±5.7	82.4±6.8	54.7±4.2
SHP-3-8	0.1±0.01	0.1±0.01	0.6±0.05	2.3±0.2	52.2±4.7	78.1±7.2	91.7±8.4	191.6±15.9
SHP-3-10	0.2±0.02	0.7±0.06	2.3±0.2	61.8±5.7	72.7±6.7	74.2±6.8	75.6±6.8	40.5±3.5
SHP-3-12	0.3±0.02	0.9±0.08	3.2±0.3	45.3±4.1	58.9±5.5	74.7±6.9	90.2±8.6	55.2±4.8
SHP-3-16	3.0±0.2	3.4±0.3	5.9±0.5	42.6±3.2	70.4±6.4	70.8±6.3	97.9±8.7	58.7±4.6

Table S3

Size (hydrodynamic diameter, using number (Num), intensity (Int) and volume (Vol) distribution in analysis, Z-Average (Z_{Aver}), polydispersity index (PDI) and Zeta potential (ZP, mV) of lipid formulations.

Formulation	SHP-2-Bn (wt %)	Loaded compound		Hydrodynamic diameter (nm)			Z_{Aver} (nm)	PDI	ZP (mV)	EE, %	LC, %
		(wt %)		Num	Vol	Int					
PC	-	-	-	51±1	68±1	106±1	99±2	0.14±0.03	-9±1	-	-
PC/SHP-2-Bn	0.5	-	-	52±0.5	39±0.4	75±0.8	65±1	0.14±0.02	+5±0.5	-	-
PC/SHP-2-Bn	1	-	-	38±1	51±1	91±1	89±1	0.21±0.04	+10±1	-	-
PC/SHP-2-Bn	2	-	-	13±2	16±1	68±1	48±1	0.31±0.01	+21±1	-	-
PC/SHP-2-Bn	5	-	-	18±1	68±1	91±1	73±1	0.23±0.02	+28±5	-	-
PC	0	SHP-2-8	0.4	75±1	108±1	131±1	112±2	0.14±0.02	+66±1	-	-
PC/SHP-2-Bn	0.5	SHP-2-8	0.4	50±1	68±1	164±1	130±2	0.24±0.01	+64±7	-	-
PC/SHP-2-Bn	0.5	SHP-2-10	0.4	56±0.5	92±0.7	130±1; 12±0.1	105±2	0.19±0.01	+74±5	81.7	21
PC/SHP-2-Bn	0.5	SHP-2-12	0.4	53±0.4	78±0.5	112±0.9	87±1	0.23±0.02	+79±5	85.5	23.8
PC/SHP-2-Bn	0.5	SHP-2-16	0.4	57±0.4	86±0.5	119±0.8	95±1	0.21±0.005	+77±5	93	27.6

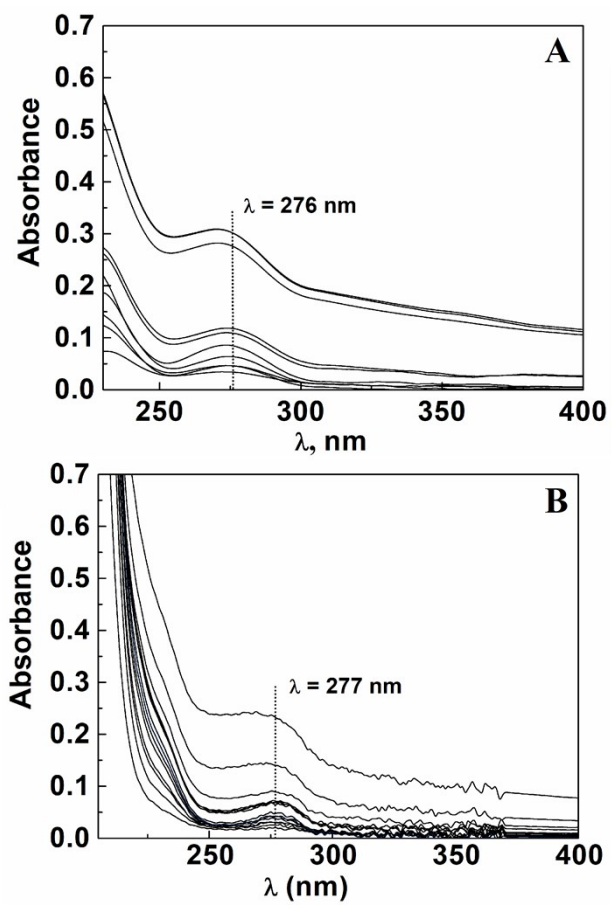


Fig. S10. Spectra of SHP-2-10 (A) and SHP-2-16 (B) in Saline (NaCl, 0.15 M) recorded during release time, pH=7.4, L=1 cm, 25°C.

Table S4

Hemolytic action against human red blood cells of SHP-s-R-loaded lipid formulations

Compounds	Hemolysis, %							HC ₅₀ , μM
	Concentration, μM							
	2	7	10	50	200	600	1000	
SHP-2-8	0	0.3±0.01	0.3±0.02	1.1±0.08	3.5±0.3	21.2±1.8	74.7±6.4	680±56
SHP-2-10	0.3±0.01	0.4±0.03	0.7±0.06	2.6±0.21	7.8±0.6	20.8±1.7	77.9±6.7	641±53
SHP-2-12	0.5±0.03	1.3±0.1	2.6±0.2	8.8±0.7	22.7±1.8	64.3±5.8	100±8.8	467±37
SHP-2-16	0.2±0.01	0.4±0.02	1.7±0.13	2.6±0.2	8.4±0.7	38.9±2.8	75.6±6.3	716±64
SHP-3-8	0.4±0.02	0.4±0.02	1.1±0.08	2.7±0.22	6.9±0.54	56.8±4.7	84.1±7.7	561±48
SHP-3-10	0	0.1±0.009	0.4±0.02	1.8±0.2	6.6±0.5	37.4±2.6	80.2±6.9	712±58
SHP-3-12	0.5±0.04	0.8±0.06	1.3±0.1	3.9±0.24	8.7±0.8	61.8±5.8	86.8±7.2	530±42
SHP-3-16	0.2±0.01	0.7±0.05	1.1±0.09	4.2±0.3	14.1±1.2	42.0±3.7	88.8±7.6	638±54

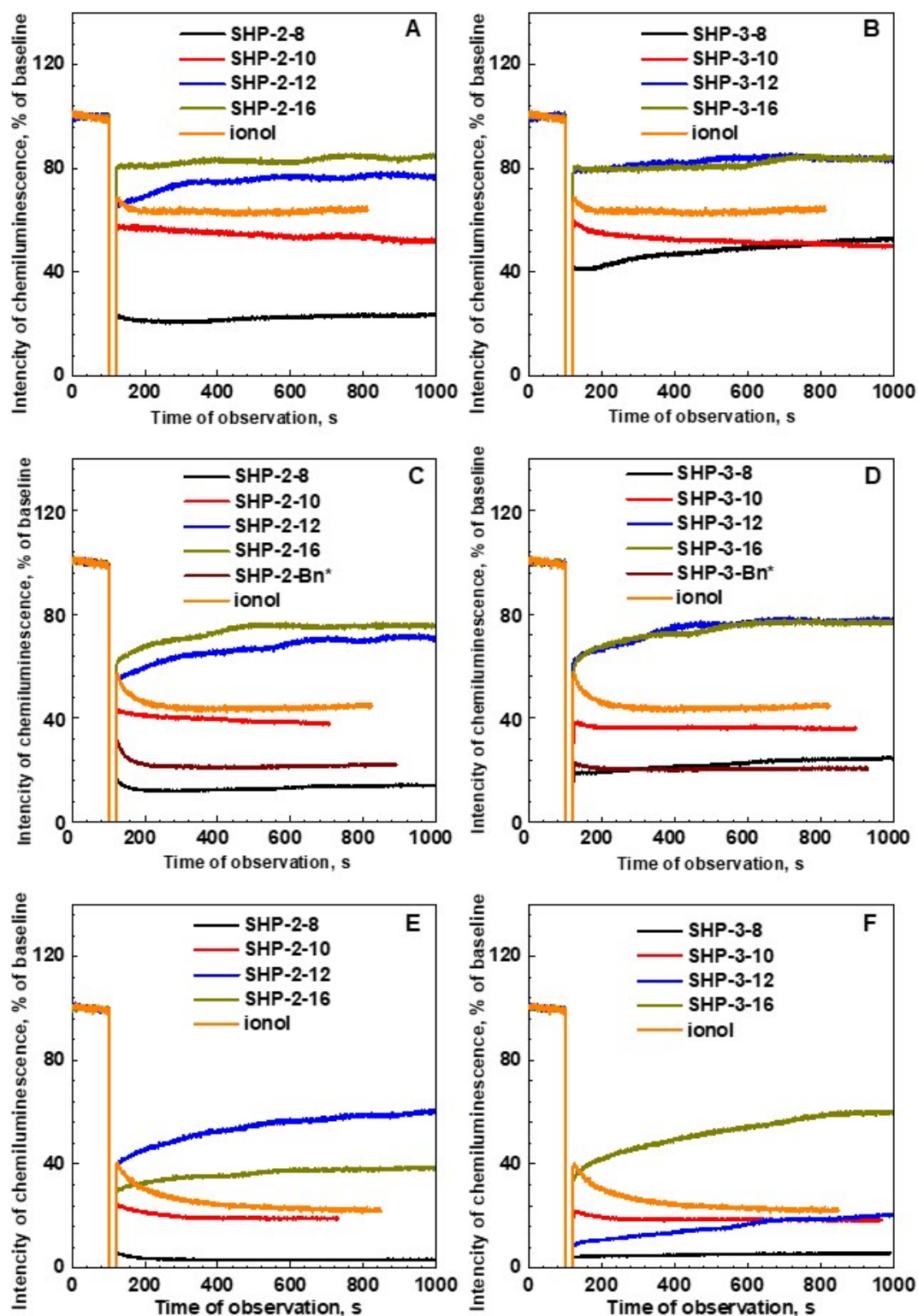


Fig. S11. Chemiluminescence intensity for ABAP and LM in a buffer solution (total volume of 1.000 mL): the area with chemiluminescence level about 100% represents the time before the addition of the test substances (baseline); the short-time fall of the curve to 0 represents the time of introduction of substances tested; the following sections of curves show the interaction of the substances with free radicals: A, C, E – for SHP-2-R (0.25; 0.5 and 1 mM solutions respectively); B, D, F – for SHP-3-R (0.25; 0.5 and 1 mM solutions respectively).

* - the results have been published in [21].

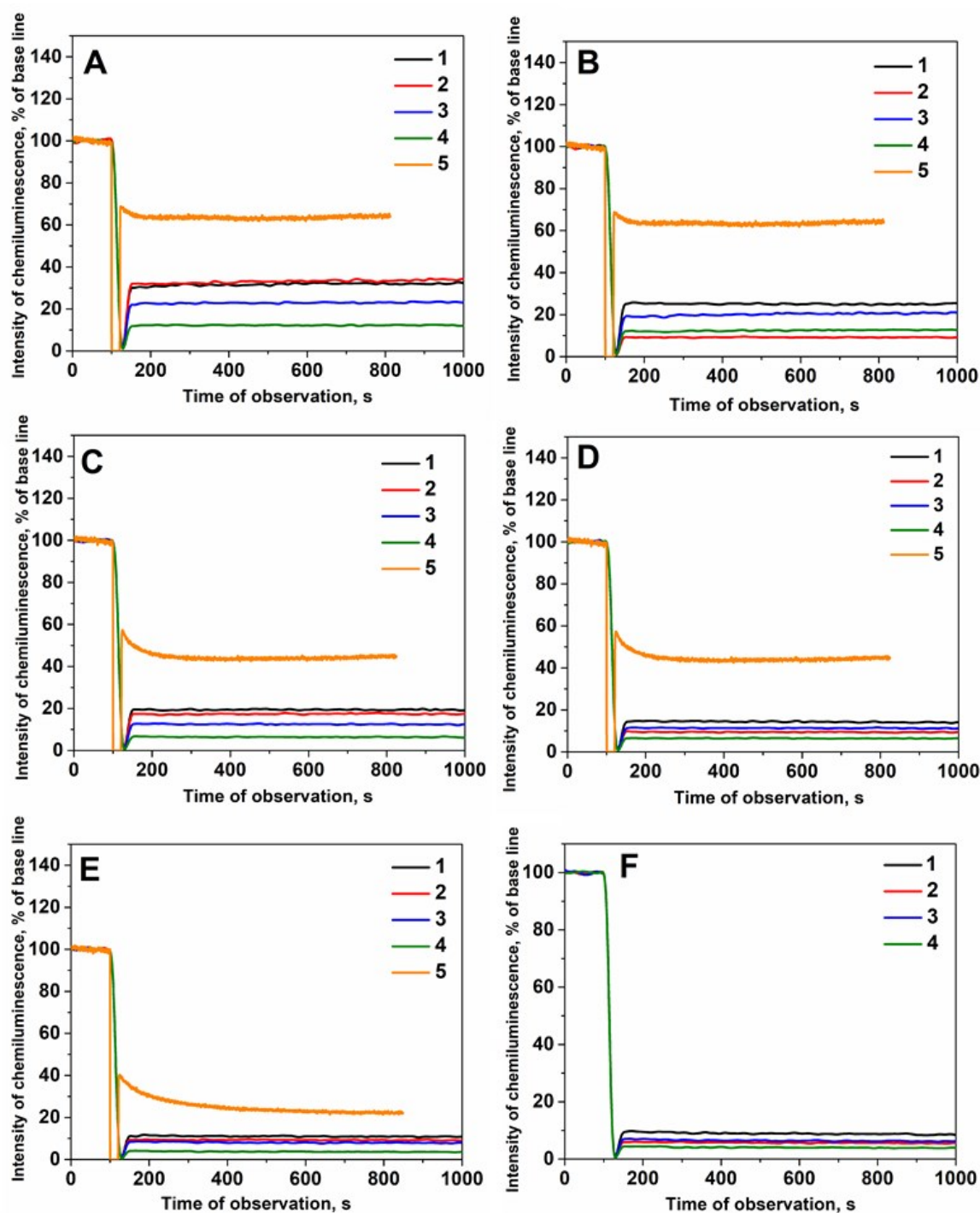


Fig. S 12. Chemiluminescence intensity for ABAP and LM in a buffer solution (total volume of 1.000 mL): the area with chemiluminescence level about 100% represents the time before the addition of the test substances (baseline); the short-time fall of the curve to 0 represents the time of introduction of substances tested; the following sections of curves show the interaction of lipid formulations with AAPH radicals: A, B (0.25mM), C, D (0.5 mM), E, F (1 mM) ; A, C, E (for SHP-2-R); B, D, F (C – for SHP-3-R) 1 – PC/SHP-2-Bn/SHP-s-8; 2 – PC/SHP-2-Bn/SHP-s-10; 3 – PC/SHP-2-Bn/SHP-s-12; 4 – PC/SHP-2-Bn/SHP-s-16; 5-ionol.